 FDMP, vol.14, no.3, pp.177-200, 2018

Experimental and Theoretical Analysis of a Novel Cascade Solar Desalination Still

M. Bouzaid[1, *], O. Ansari[1], M. Taha-Janan[1] and M. Oubrek[1]

Abstract: Ocean water is characterized by very high salinity, which generally makes it unsuitable for human or animal's needs. The production of potable water from the ocean, therefore, requires a desalination process, which is often regarded as the crucial limitation to overcome towards widespread use of ocean water as the primary source of water for human consumption. In this study, we analyze both experimentally and theoretically the thermal performances and productivity of a solar still based on a novel form of absorber plate. The related system of energy equations consists of five heat exchange relationships in the form of first differential equations, which we solve using a proper numerical method (implemented using the C++ language). The new still performances predicted theoretically are compared with experimental results for several cases and conditions.

Keywords: Desalination, solar still, basin type solar still, cascade solar still, brackish water.

Nomenclature

A	Area, m^2
L	Length, m
Cp	Specific heat, J $Kg^{-1}K^{-1}$
h	Heat transfer coefficient, W $m^{-2}K^{-1}$
I_G	Incident solar power, W m^{-2}
Q	Heat flux density, W m^{-2}
m	Mass, kg
t	Temps, hour
dt	Calculation step, hour
T	Temperature, °C
dT	Incremental rise, °C
ΔT	Temperature difference, °C

Greek letters

ε	Emissivity
α	Absorptivity

[1] Laboratoire de Mécanique Appliquée et Technologies, Centre de Recherche en Sciences et Technologies Industrielles et de la Santé, ENSET, Mohammed V University in RABAT, Avenue de l'Armée Royale, BP 6207 Rabat-Instituts, Morocco.

[*] Corresponding Author: M. Bouzaid. Email: mariambouzaid.91@gmail.com.

τ	Transmissivity
λ	Thermal conductivity, $\mathrm{Wm^{-1}K^{-1}}$
ρ	Density, $Kg.\mathrm{m^{-3}}$
β	Coefficient of thermal expansion, 1/K
υ	kinematic viscosity air, m^2/s

Subscripts

a	Ambient
air	Air
b	Absorber
bH	Horizontal surface of absorber plate
bi	Inclined surface of absorber plate
c	Convection
cd	Conduction
e	Evaporation
e,is	External face of insulation
g	Glass
is	Insulation
i,is	Internal face of insulation
r	Radiation
sky	Sky
w	Brackish water

1 Introduction

Water is a most essential element for life, however, one-third of the world's population suffers from water scarcity. 97% of planet's water resides in the ocean. Only 3% of water coverage is fresh, with less than 1% of this water is usable by humans [Gleck (1996)]. The need for potable water in the world is continuously increased day by day because of industrial, population and agricultural growth. Currently, the problem of scarcity threatens even regions that considered water-rich [Shannon, Bohn, Elimelech et al. (2008)]. One of the most serious problems afflicting people is that fresh and clean water resources are unevenly spread in many countries in the world. According to Shannon et al. [Shannon, Bohn, Elimelech et al. (2008)] the many problems worldwide associated with the lack of clean, fresh water are well known: 1.2 billion people suffer from lack of access to clean drinking water and more than millions of people die annually from diseases transmitted through unsafe water or human excreta.

Morocco is faced to very limited water resources in addition to an uneven distribution and under more pressure due to a combination of population growth, economic development and a strong decline in precipitation [Choukr-Allah (2011)]. According to United Nations World Water Development Report 2016 and Choukr-Allah [Choukr-Allah (2011)], the water availability in Morocco has decreased from 3,500 m^3 per person per year in 1960 m^3 to 1,000 m^3 in 2000, and forecasts are predicting it will fall to 490 m^3 in 2020. To overcome the problem of water shortage, there is a demand for some

technique that can be used for purifying of brackish and salt water for drinking purposes. For this reason, several researches are conducted to invent robust new methods of producing water at a lower cost, with less energy and respect the environment. Producing clean water using clean energy, also improving the efficiency of water source technology is considered as the main challenge for many researchers.

Solar desalination represents an interesting way for drinkable water production by using a clean energy for the following reasons: First, 97% of earth's water is salty [Gleck (1996)]. Second, Morocco has an important solar energy potential. According to Nfaoui et al. [Nfaoui and Sayigh (2015)], the annual number of sunshine hours is relatively high and reaches 3405 h as well as, the values of irradiation that are 7.22 $kWh/m^2/day$ for direct normal and 5.86 $kWh/m^2/day$ for global irradiation. Third, solar energy is a free pollution energy source, compared to other commonly used sources. There are many techniques of desalination processes which can be classified into indirect and direct solar technologies. Indirect desalination uses solar energy indirectly, in these systems solar energy is collected by using non-concentrating or concentrating solar thermal collectors or photo-voltaic panels. There are two types of indirect process- Membrane and thermal distillation. Membrane distillation (MD) or Reverse Osmosis (RO) methods based on the principle of osmosis to remove salt, by using a series of semi-permeable membranes.

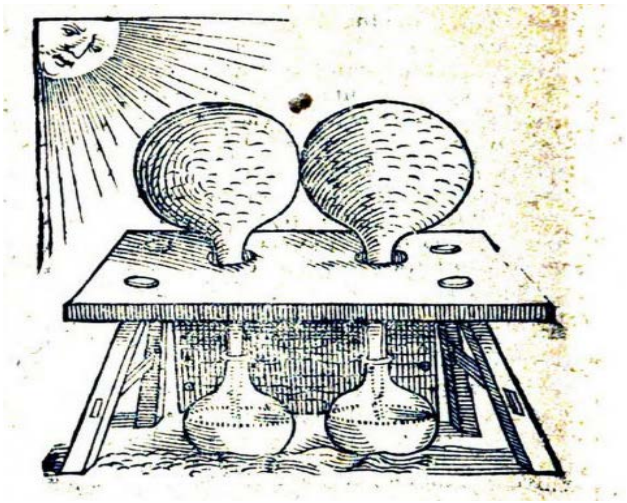

Figure 1: Direct solar desalination according to Della Porta [Della Porta (1608)]

Thermal technologies such as Multi Stage Flash (MSF), Multiple Effect Distillation (MED), Thermal Vapor Compression (TVC) processes use heat to evaporate saline water and condense water vapor to collect freshwater. A review of indirect solar desalination is given by Ali et al. [Ali, Fath and Armstrong (2011)]. Direct solar still utilizes solar radiation directly. In 1608 as shown in Fig. 1 Della Porta [Maurel (2006)], has illustrated the first direct desalination process used by Greek sailors in the 4th century BC to evaporate seawater and create drinking water. This type of desalination is the oldest and the simplest process. With respect to the other types of desalination, direct solar still is

the best technology because it's cheap, less complicated, can be easily fabricated and installed in rural areas However many researchers indicate that the efficiency, as well as the production rate of the direct solar still is very low compared to other desalination processes [Abujazar, Fatihah, Rakmi et al. (2016)]. For this reason, several researches have been carried out to increase the efficiency and the performance of this type of solar stills.

A summary of the available water desalination technologies is mentioned in Tab.1. For more information please see the review given by Ali et al. [Ali, Fath and Armstrong (2011)] for the indirect processes and for the direct processes [Mohammed Shadi Abujazar, Fatihah et al. (2016)].

Table 1: Direct and Indirect solar desalination processes

Solar Thermal Desalination	Indirect Processes	Humidification & Dehumidification	
		Membrane Distillation (MD)	
		Reverse Osmosis (RO)	
		Multi Stage Flash (MSF)	
		Multi Effect Desalination (MED)	
		Vapor Compression (VC)	
	Direct Processes	Solar Stills	Active
			Passive

As shown in Fig. 2 the desalination process in a conventional solar still is given in our article published in 2016 [Bouzaid, Oubrek, Ansari et al. (2016)] and is processed in 3 steps:

(1) Received solar radiation is absorbed by the plate in painted black metal. Heat is then transferred by convection to the water in the basin. The absorber plate temperature and the saline water temperature can reach more than 60°C.

(2) An evaporation of water results from the increase of its temperature. The water vapor rises upward on the sloping glass cover.

(3) The low temperature of the glass cover surface facilitates the condensation of the water vapor. The maximum value of the glass cover temperature can reach 40°C.

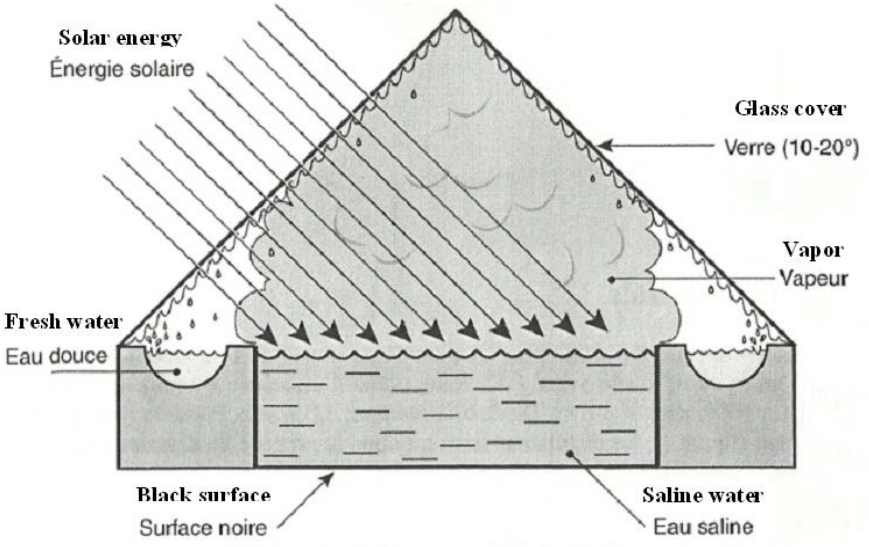

Figure 2: Conventional solar still process indicated by Maurel [Maurel (2006)]

Our pattern is registered in the same objective of improving the production rate of solar still. As is shown in Fig. 3 the device consists of a cascade basin with inclined absorber plates and baffles in the external face.

Figure 3: Cascade solar still with inclined absorber plate and baffles

1.1 Performance improvement techniques for the solar still

According to several researchers such as Singh et al. [Singh and Tiwari (1991); Maurel (2006); Sharshir, Yang, Peng et al. (2015)], solar still is an excellent device of producing fresh water from saline water. It is one of the simplest applications for solar desalination, in addition to being clean and technically easy to proceed and maintain. Due to its limited productivity, it is not widely used. Many researchers have proposed new structures which have been tested theoretically and experimentally. The reasonable quantity of freshwater can be produced via a cheap and a robust solar still in areas that have an important solar

potential. The simplest and the cheapest type of solar still is the basin type. A digital simulation has developed by Cooper [Cooper (1969)] to evaluate a solar still performance. The simulation results indicate that water depth has little effect on productivity. Tiwari et al. [Tiwari and Madhuri (1987)] showed similar results of Cooper and proved that there is a decrease in daily yield, about 44%, by changing water depth from 0.01 m to 0.20 m when the temperature is at 40°C and the yield of a solar still is maximum for a brine temperature of more than 45°C. In 2005 a transient mathematical model is presented by El-Sebaii [El-Sebaii (2005)] for a solar still with three basins. Numerical calculations were shown that the lower basin productivity is better than the middle and upper basins productivities.

It is found that the productivity of the still increases with the increase of wind velocity and it equals 12 $kg/m^2/d$ with a maximum solar intensity of 1057 W/m^2. Inclined solar still has an inclined absorber plate with an angle according to the horizontal surface. The inclined solar still form offering a longer flow of feed water on absorber plate to increases the rate of evaporation. Aybar [Aybar (2006)] designed and tested an inclined solar still using the bare plate, black-cloth wick and black fleece wick. The results indicate that the wicks are better than bare plate because they increased the fresh water by two or three times. The average hot water temperature collected on the tank was about 40°C. According to Tiwari et al. [Tiwari and Madhuri (1987)], the water deepness is inversely proportional to the still productivity. Guarding the least deepness of brine in a solar still is very difficult. Stepped solar still is a robust technique to purifying saline water and used by a lot of researchers to achieve a minimum water depth in the basin. Radwhan [Radwhan (2004)] presents a transient analysis of a stepped solar still, consists of five basins for heating and humidifying agriculture greenhouses (GH). The daily average efficiency of the still can reach 63% and the total daily yield is about 4.92 L/m^2. Velmurugan et al. [Velmurugan, Kumar, Haq et al. (2009)] fabricated and tested a stepped solar still of 50 trays. Sponges and fins used aiming the productivity improvement of the solar still and they improved the output by nearly 98%. Kabeel et al. [Kabeel, Khalil, Omara et al. (2012)] used a modified stepped solar still consists of the number of trays with different widths and depths to improve the performance of solar still.

1.2 Factors influencing the productivity

There are various factors control the output rate in the solar stills. The metrological parameters cannot be controlled however the difference between water and the glass temperatures, areas of water free surface and absorber plate, the value of the inlet water temperature, the glass orientation and the depth of water can be changed to increase the stills production.

- Water-glass temperature difference

Increasing the temperature difference between the glass cover and the basin water leads to an increase in the evaporative and the convective heat transfer from basin water to glass cover [Sharshir, Yang, Peng et al. (2015)].

- Free surface area of water and deepness of water

The water evaporation rate in the basin is directly proportional to the water areas. For this reason the free surface area of the water in the basin must be increased to improve the solar still production [Sharshir, Yang, Peng et al. (2015)].

In 2008, Velmurugan et al. [Velmurugan and Srithar (2008)] evaluated the effect of using fins inside the solar still. The fins increase the free surface area of the water. The maximum accumulated fresh water from the solar still was about $2.2\ \mathrm{kg/m^2}$ [Sathyamurty, Samuel and Nagarajan (2015)]. In 1987, Tiwari [Tiwari (1987)] studied theoretically and experimentally the effect of water depth on a solar still. This study indicates that the yield of solar still increases with a decrease in water depth when the water is at temperature of 40°C. The depth of the brackish water in the still is inversely proportional to the production rate. As a result the productivity reaches the maximum for the least water deepness [Sharshir, Yang, Peng et al. (2015)].

- Absorber plate area

For augmenting the evaporation rate, several geometries of absorber plate are proposed, fabricated and tested, which could maintain minimum depth in the basin and enhance the productivity [Velmurugan, Kumar, Haq et al. (2009)].

- Temperature of inlet water

The water evaporation rate in the solar still is directly proportional with the temperature of the water free area (inlet water temperature) [Sharshir, Yang, Peng et al. (2015)].

- Angle of the glass cover

The glass cover is an important component in the solar still. It constitutes a condensing surface of the steam and a transmission surface of the radiation. Better angle of inclination provide a better performance and facilitate the runoff of condensed water. Singh et al. [Singh and Tiwari (2004)] signalized that the annual solar still yield reached a maximum value if the glass cover inclination angle is set equal to the place latitude.

2 Targets and methodology

Several designs have been developed to enhance the efficiency of the single basin type. The stepped solar stills have higher productivity compared with basin-type stills, because the absorber plate is split into a number of steps, offering minimum depth of brine water. In this present work, a novel form and construction of stepped solar still was proposed, tested and fabricated. The new conception of the still consisted of a stepped absorber with alternated plate and sloped surfaces and baffles. This new geometry of the absorber plate area increases the difference between the glass cover and the basin water temperatures and minimizes the depth of water. It also uses baffles to increase the inlet water temperature at each step. A mathematical model and thermal analysis were formulated in order to investigate the performance of the modified stepped solar still. A numerical code was developed in C++ program, tested and used to carry on the present study.

The results obtained using the elaborated model are validated by comparison to available experimental data collected on 27, 28 and 29 of March 2017 at the Higher Normal School of Technical Education (ENSET) of Rabat-Morocco.

3 System description

3.1 Stepped solar still process

The present work is an extension of first attempt of modeling the new device by Bouzaid et al. [Bouzaid, Oubrek, Ansari et al. (2016)]. The absorber plate of the stepped still is in the form of stairs made of a number of steps. The absorber plate and basin temperatures are higher than those of the single basin still. Two reasons are at the origin of this difference:

(1) The trapped air in the stepped stills is heated much faster than the conventional still because they have a smaller air volume.

(2) According to Abdallah et al. [Abdallah, Badran and Abu-Khader (2008)] the step-wise basin provides higher heat and mass transfer surface area than the flat basin. This consequently leads to increase the basin water temperature of stepped solar still.

3.2 Novel stepped solar still design

As we indicate in Bouzaid et al. [Bouzaid, Oubrek, Ansari et al. (2016)]. Fig. 4 shows, the classical ordinary form of cascade solar still has plate absorber with horizontal and vertical surfaces; the angle between the two surfaces is about 90°. In the new design the glass cover and the vertical surface of absorber plate are inclined with angles of 25° and 35° respectively for better orientation relative to the sun. The Absorber plate inclination was equal to the latitude of Rabat (34°47'N).

Our pattern as shown in Fig. 5 consists of horizontal and vertical/inclined types of absorber plates and the angle between the two surfaces was about 145°. In order to improve the performance of cascade solar still, the water transit time on the absorber plate should be maximized. Therefore in the new design of slope absorber plate we added different weirs to the surface of absorption.

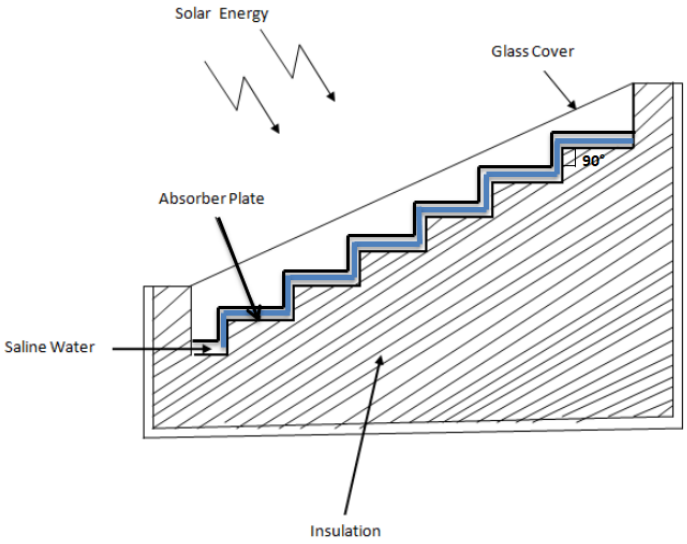

Figure 4: Schematic sketch of a stepped solar still

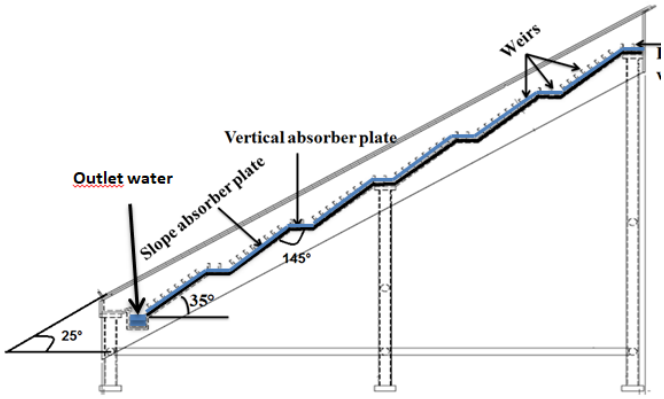

Figure 5: Schematic sketch of the new stepped absorber plate (with slope surface and weirs)

3.2.1 Solar still construction

The different elements of our pattern are explained in our previous work Bouzaid et al. [Bouzaid, Oubrek, Ansari et al. (2016)] and presented in the Fig. 6:

- Glass cover technology

The solar still has a top cover made of glass. The glass cover has two functions:

First, the glass cover is a selective filter of solar radiation. Then the absorber plate inside the solar still absorbs the radiations.

Second, the glass cover presents a condensing surface of the steam, for this purpose, a good wettability is necessary.

We used inclined glass cover (more than 25°) for two reasons:

- To provide better orientation relative to the incident radiation
- To facilitate the runoff of condensed water to the collector

3.2.2 Basin technology

The basin is made of metal (aluminum); thermal insulation is achieved by a coating inside the basin. The basin bottom sealing is achieved by a synthetic rubber covering mat. The absorber plate is made of aluminum and painted black. It consists of horizontal and sloped surfaces with black metal baffle on the inner face.

The new construction of the absorber plate presents the following advantages:

- Better absorption of solar radiation
- Minimum depth of water
- Quick water Heating

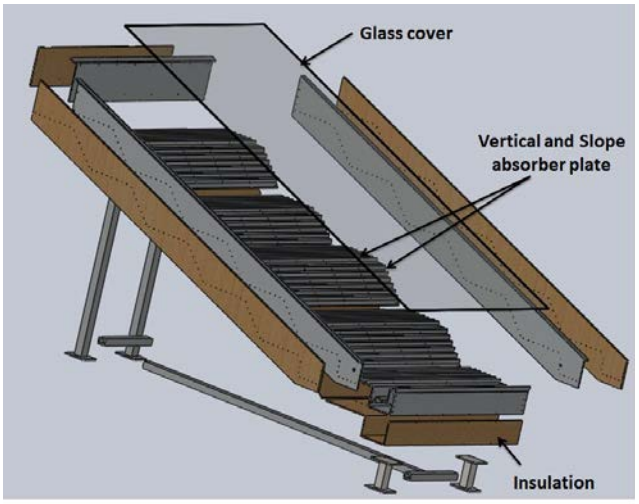

Figure 6: Different elements of new design for cascade solar still

4 Mathematical model

The energy balance for the stepped solar still will be applied to five levels: glass cover, saline water, absorber, inner and external face of insulation. The temperatures of the glass cover, saline water, absorber plate and insulation material can be evaluated at every instant. The Energy balance equations are used for determining the temperatures of the elements of the solar still. They are written under the following assumptions:

- Heat losses from the sides of the solar still are neglected.
- Absence of air leakage from the still
- The cover is clean.
- Uniform temperatures of each component.
- Uniform temperatures, equal to the ambient temperature are set for all the elements at the beginning of the process.
- Condensation occurs only on the cover.
- The glass has good moisture.
- The concentration of the saline water is not implicated in the heat and mass transfer.
- The whole device is leak-free.

The energy balance equations are solved for all the elements of the device and water to obtain the analytical results.

In these equations, T_g, T_w, T_b and T_{is} represent respectively the average temperatures of the glass cover, the brine water, the absorber plate and insulation expressed in degrees Celsius.

4.1 Mathematical expressions of the energy balance for the solar still

4.1.1 Thermal energy balance of the condensing glass cover

The thermal energy balance for the glass cover is expressed as follows:

$$C_{pg}m_g\frac{dT_g}{dt} = Q_{rwg} + Q_{cwg} + Q_{ewg} + Q_{cbg} - Q_{rgsky} - Q_{cga} + P_g \quad (1)$$

The radiative heat exchange between the glass cover and the sky is given by the following expression of the flux density:

$$Q_{rgsky} = h_{rgsky}A_g(T_g - T_{sky}) \quad (2)$$

h_{rgsky} representing the radiative heat exchange coefficient between the two considered elements and is calculated using Stefan Boltzmann law:

$$h_{rgsky} = \sigma\varepsilon_g(T_g^2 + T_{sky}^2)(T_g + T_{sky}) \quad (3)$$

The expression considered for the sky temperature is [Duffie and Beckman (1980)]:

$$T_{sky} = 0.0552(T_a{}^{1.5})$$

The heat flux density for convective exchange between the glass cover and the ambience is given by:

$$Q_{cga} = h_{cga}A_g(T_g - T_a) \quad (4)$$

The convective heat exchange coefficient h_{cga} can be determined following [Kreith (1967); Tiwari (2002); Dashtban and Tabrizi (2011)] by:

$$h_{cga} = 5.3 + 3.8V \quad (5)$$

Where V represents a wind velocity average.

The flux density of the radiative exchange between the brackish water and the glass is the following expression:

$$Q_{rwg} = h_{rwg}A_w(T_w - T_g) \quad (6)$$

Where h_{rwg}, the radiative heat exchange coefficient is found using Stefan-Boltzman law, and then have the expression:

$$h_{rwg} = \frac{\sigma(T_w^2+T_g^2)(T_w+T_g)}{\frac{1}{\varepsilon_w}+\frac{1}{\varepsilon_g}-1} \quad (7)$$

ε_w and ε_g are respectively the brackish water and the glass cover emissivity and σ is the Stefan-Boltzman constant.

The convective heat flux density between the brackish water and the glass cover is expressed by:

$$Q_{cwg} = h_{cwg}A_w(T_w - T_g) \quad (8)$$

The expression of the heat exchange coefficient h_{cwg} is determined by the expression suggested by Kumar et al. [Kumar and Tiwari (1985); Aggarwal and Tiwari (1998); Tiwari and Tiwari (2006)] and is then:

$$h_{cwg} = 0.884[T_w - T_g + \frac{(P_w-P_g)(T_g+273.15)}{268.9\,10^3-P_w}]^{1/3} \quad (9)$$

The expression of the evaporative heat flux density between the brackish water and the glass cover is given by:

$$Q_{ewg} = h_{ewg} A_w (T_w - T_g) \tag{10}$$

The involved evaporative heat exchange coefficient h_{ewg} is determined, following According to Dunkle et al. [Dunkle (1961); Tiwari, Lawrence and Gupta (1989); Dashtban and Tabrizi (2011)], using the following expression:

$$h_{ewg} = 16.273\ 10^{-3} h_{cwg} \frac{(P_w - P_g)}{(T_w - T_g)} \tag{11}$$

P_w and P_g representing the water vapour pressures at the brackish water and the glass cover respectively, and are suggested by Tiwari [Tiwari (2002)], as follows:

$$P_w = \exp(25.317 - \frac{5144}{T_w + 273.15}) \tag{12}$$

$$P_g = \exp(25.317 - \frac{5144}{T_g + 273.15}) \tag{13}$$

The convective heat flux density between the glass cover and the inclined surfaces of absorber plate is expressed by:

$$Q_{cbg} = h_{cbg} A_{bi} (T_b - T_g) \tag{14}$$

According to Hollands et al. [Hollands, Unny, Raithby et al. (1976); Sathyamurthy, Samuel, Nagarajan et al. (2015)], the convective heat exchange coefficient for an inclined surface is correlation between Nusselt number (Nu) and thermal conductivity of air λ_{air} .

$$Nu = 1 + 1.44 \left[1 - \frac{1708}{R_{aH} \cos\theta}\right] \left[1 - \frac{1708\ (\sin 1.8\ \theta)^{1.6}}{R_{aH} \cos\theta}\right] + \left[\left(\frac{RaH \cos\theta}{5830}\right)^{1/3} - 1\right] \tag{15}$$

Rayleigh number is expressed as:

$$R_{aH} = \frac{g\ \beta\ (T_b - T_g)}{\nu\ \alpha_{air}} \tag{16}$$

Where $\beta = \frac{1}{T_b + 273.15}$ and α_{air} is the diffusivity of air.

The convective heat transfer co-efficient between glass cover and inclined surfaces of absorber plate

$$h_{cbg} = \frac{Nu\ \lambda_{air}}{Lbi} \tag{17}$$

The fraction of the incident radiation heat flux density absorbed by the glass cover of the solar still P_g is calculated by:

$$P_g = I_G A_g \alpha_g \tag{18}$$

4.1.2 Thermal energy balance of the brackish water

Thermal energy balance for the brackish water is expressed by:

$$C_{pw} m_w \frac{dT_w}{dt} = Q_{cbw} - Q_{rwg} - Q_{cwg} - Q_{ewg} + P_w \tag{19}$$

The expression of the heat flux density exchanged between the horizontal surfaces of absorber plate and the brackish water is:

$$Q_{cbw} = h_{cbw} A_{bH} (T_b - T_w) \quad (20)$$

Where h_{cbw} is the convective heat exchange coefficient between the absorber plate and the brackish water. It is calculated using the correlation of Nusselt number [Kreith (1967); Ansari, Asbik, Bah et al. (2003)].

For $Gr < 10^5$. Nu=1

$$h_{cbw} = \frac{\lambda_w}{L_{bH}} \quad (21)$$

If $10^5 < Gr < 2\ 10^7$

$$Nu = 0.54(Gr\ Pr)^{0.25} \quad (22)$$

$$h_{cbw} = \frac{Nu\ \lambda_w}{L_{bH}} \quad (23)$$

If $Gr > 2\ 10^7$

$$Nu = 0.14(Gr\ Pr)^{0.25} \quad (24)$$

$$h_{cbw} = \frac{Nu\ \lambda_w}{L_{bH}} \quad (25)$$

Gr, Nu and Pr designate respectively the non-dimensional Grashof, Nusselt and Prandlt numbers.

The solar radiation P_w absorbed by the brackish wateris given by:

$$P_w = I_G A_w \alpha_w \tau_g \quad (26)$$

4.1.3 Thermal energy balance of the absorber plate

The thermal energy balance for the absorber plate is expressed by:

$$C_{pb} m_b \frac{dT_b}{dt} = -Q_{cbw} - Q_{cd} - Q_{cbg} + P_b \quad (27)$$

The conductive heat flux density of the basin is expressed by:

$$Q_{cd} = \frac{\lambda_b}{e_b} A_b \left(T_b - T_{i,ins}\right) \quad (28)$$

λ_b and e_b respectively denote the thermal conductivity and thickness of the absorber plate.

The solar power absorbed by the basin liner P_b is expressed by:

$$P_b = P_{bH} + P_{bi} \quad (29)$$

Where:

P_{bH} is the solar power absorbed by the horizontal surfaces of the absorber plate.

P_{bi} is the solar power absorber by the inclined surfaces of the absorber plate.

$$P_{bH} = I_G A_{bH} \alpha_b \tau_g \tau_w \quad (30)$$

$$P_{bi} = I_G A_{bi} \alpha_b \tau_g \quad (31)$$

4.1.4 Inner face of insulation material

The thermal energy balance for the inner face of insulation is expressed by:

$$C_{p,ins} m_{ins} . \frac{dT_{i,ins}}{dt} = - Q_{cd,ins} + Q_{cd} \quad (32)$$

The expression of the conductive heat flux density of the insulation material is given by:

$$Q_{cd,ins} = \frac{\lambda_{ins}}{e_{ins}} A_{ins} \left(T_{i,ins} - T_{e,ins} \right) \quad (33)$$

λ_{ins} and e_{ins} respectively denote the thermal conductivity and thickness of the insulation material.

4.1.5 External face of insulation material

The thermal energy balance for the external face of insulation is calculated under the following expression:

$$C_{p,ins} m_{ins} \frac{dT_{e,ins}}{dt} = -\left(Q_{r,ia} + Q_{c,ia} \right) + Q_{cd,ins} \quad (34)$$

The radiative heat flux density between the insulation material and the ambient air is presented by:

$$Q_{r,ia} = h_{r,ia} A_{ins} (T_{e,ins} - T_a) \quad (35)$$

The radiative heat exchange coefficient $h_{r,ia}$ is calculated by Stefan Boltzmann law.

$$h_{r,ia} = \sigma \varepsilon_i \left(T_{e,ins}^2 + T_a^2 \right) \left(T_{e,ins} + T_a \right) \quad (36)$$

The convective heat flux density between the external face of insulation and the ambience is expressed by:

$$Q_{c,ia} = h_{c,ia} \left(T_{e,ins} - T_a \right) \quad (37)$$

The convective heat exchange coefficient h_{cwg} between the insulation and the ambient air is given by:

$$h_{c,ia} = 1.78 \times \left| T_{e,ins} - T_{sky} \right|^{0.25} \quad (38)$$

4.1.6 Hourly productivity

According to El-Sebaii et al. [El-Sebaii, AL-Ghamdi, Al-Hazmi et al. (2009)] and Dashtban et al. [Dashtban and Tabrizi (2011)], the hourly distillate output from a solar still can be calculated as:

$$m'_{ew} = h_{ewg} . A_w . \left(T_w - T_g \right) / Lv$$

Where Lv is the latent heat of vaporization of water.

4.2 Analytical expression of the glass cover, saline water, absorber plate and insulation temperatures

The formalism obtained consists in a system of five differential equations which takes the following form:

$$\frac{dT}{dt} + X(t).T = \beta(t) \tag{39}$$

$$X = \begin{cases} x_1 = \dfrac{h_{rgsky}A_g + h_{cga}A_g + h_{rwg}A_w + h_{cwg}A_w + h_{ewg}A_w + h_{cbg}A_{bi}}{C_{pg}M_g} \\ x_2 = \dfrac{\left(h_{rwg}A_w + h_{cwg}A_w + h_{ewg}A_w + h_{cbw}A_{bH}\right)}{C_{pw}M_w} \\ x_3 = \dfrac{h_{cbw}A_{bH} + {\lambda_b A_b}/{e_b} + h_{cbg}A_{bi}}{C_{pb}M_b} \\ x_4 = \dfrac{\frac{\lambda_{ins}}{e_{ins}}A_{ins} + \frac{\lambda_b}{e_b}A_b}{C_{p,ins}M_{ins}} \\ x_5 = \dfrac{\left(h_{ria} + h_{cia} + {\lambda_{ins}}/{e_{ins}}\right)A_{ins}}{C_{p,ins}M_{ins}} \end{cases}$$

$$\beta = \begin{cases} \beta_1 = \dfrac{1}{C_{pg}M_g} * (h_{cga}A_gT_a + h_{rgsky}A_gT_{sky} + \\ \left(h_{rwg}A_w + h_{cwg}A_w + h_{ewg}A_w\right)T_w + h_{cbg}A_{bi}T_b + P_g) \\ \beta_2 = \dfrac{1}{C_{pw}M_w} * \left(\left(h_{rwg}A_w + h_{cwg}A_w + h_{ewg}A_w\right)T_g + h_{cbw}A_{bH}T_b + P_w\right) \\ \beta_3 = \dfrac{1}{C_{pb}M_b} * (h_{cbw}A_{bH}T_w + h_{cbg}A_{bi}T_g + \dfrac{\lambda_b}{e_b}A_bT_{i,ins} + P_b) \\ \beta_4 = \dfrac{1}{C_{p,ins}M_{ins}} * (\dfrac{\lambda_{ins}}{e_{ins}}A_{ins}T_{e,ins} + \dfrac{\lambda_b}{e_b}A_bT_b) \\ \beta_5 = \dfrac{1}{C_{p,ins}M_{ins}} * (\dfrac{\lambda_{ins}}{e_{ins}}A_{ins}T_{i,ins} + \left(h_{ria} + h_{cia} + {\lambda_{ins}}/{e_{ins}}\right)A_{ins}T_a) \end{cases}$$

The analytical results are obtained by solving the differential equations using the analytical resolution method.

The first differential equation is solved taking into account the initial condition T_0 and the solution is expressed by:

$$T_{i+1} = \left({\beta}/{X}\right) \times \left(1 - e^{-Xt}\right) + \left(T_0 e^{-Xt}\right) \tag{40}$$

The different temperatures have been programmed and calculated numerically by iteration, using C++ simulation program.

The theoretical analysis is investigated and validated through the experimental data. T_a, T_a+1, T_a+2 and T_a are, respectively, the first iteration glass temperature, saline water temperature, absorber plate temperature and Insulation. The increase in glass temperature (dT_g), saline water temperature (dT_w), absorber temperature (dT_b), inner face of insulation ($dT_{i,ins}$), and the external face of insulation ($dT_{e,ins}$) are computed by solving the equation system obtained. This iteration is performed for a total duration of 11 hours. For the next time step, the parameter is redefined as, $T_g = T_g + dT_g$, $T_w = T_w + dT_w$, $T_b = T_b + dT_b$, $T_{i,is} = T_{i,is} + dT_{i,is}$ and $T_{e,is} = T_{e,is} + dT_{e,is}$.

Physical parameters used in theoretical calculation are shown in Tab. 2.

Table 2: Physical properties of the solar still components

	Specific Heat C_p (J $Kg^{-1}K^{-1}$)	Thermal Conductivity λ (W/m K)	Thickness e(m)
Glass Cover	800	1.02	0.005
Brackish Water	4190	0.67	0.01
Absorber Plate	896	230	0.002
Insulation	1300	0.026	0.05

5 Experimental process

In the experimental set up, as shown in Fig. 7, a cascade slope solar still with baffles connected to a saline water tank. The solar still is fed by 25 liters of brackish water with a mass salinity of 20 g per litter. The duration of the experimental process was about 11 h. It was started at 7 am and completed at 5 pm. 6 thermocouples are installed at the absorption surface and 3 on the external face of glass cover to measure the glass cover and the absorber plate temperatures during 3 days for duration of 11h/day.

Figure 7: Cascade solar still with slope absorber plate with baffles (Fabricated at the Higher Normal School of Technical Education in Rabat)

In this study, we consider the hourly variations of solar intensity and the ambient temperature relative to Rabat- Morocco city (34°47'N). These practical data were collected on 27, 28 and 29 of March 2017 at the Higher Normal School of Technical Education in Rabat.

6 Experimental and thermal results and discussion

Fig. 8 illustrates the hourly variation of the absorber pate temperature measured and the solar radiation data collected on 27 March 2017.

As it can be seen from the illustrations, the behavior absorber plate temperature has the same variation of solar intensity. The absorber plate temperature has shown in the Fig. 8 increases with an increase of solar radiation. In addition it can be observed from the Fig. 8 that the maximum of absorber plate temperature occurs at maximum of solar insulation.

Also the absorber plate temperature can reach 68.5°C for $873\,\mathrm{W.m^{-2}}$ of solar intensity which is an important value of temperature in comparison with other solar stills results.

The quality of the simulation model adopted in this study must be insured. Also its capability of providing the main characteristics of the solar still has to be confirmed. For this reason a comparison between the elaborated program results and the experimental results was interpreted.

Fig. 9 illustrates the hourly variation of the ambient temperature and the solar radiation used in the simulation and collected on 27 March 2017.

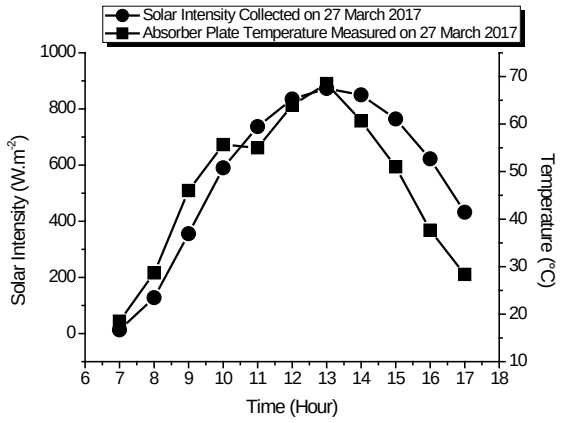

Figure 8: Hourly variation of solar radiation and the absorber plate temperature measured on the 27 March 2017

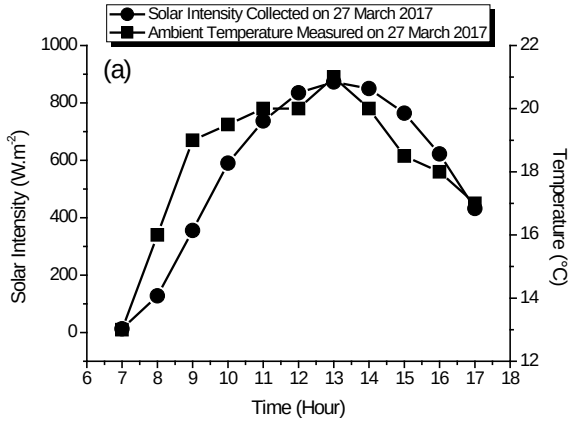

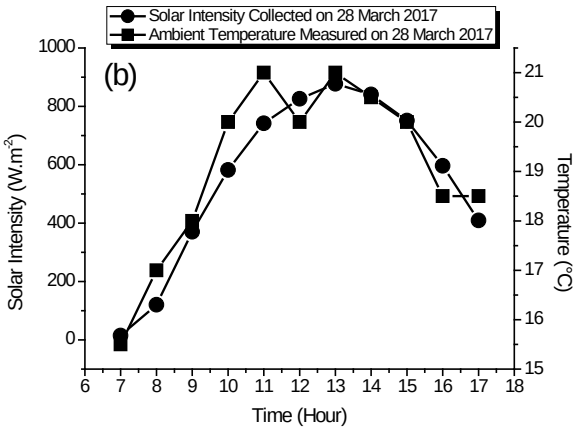

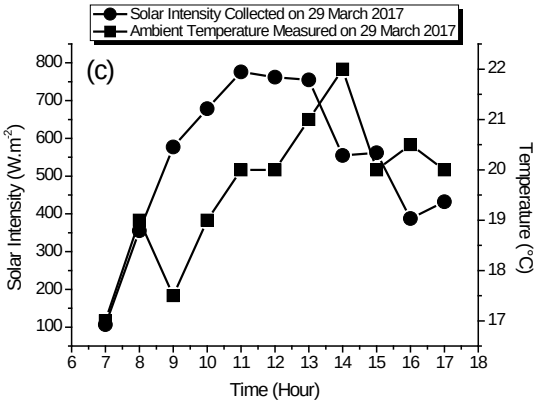

Figure 9: Hourly variation of solar radiation and the ambient temperature (Ta) used in the simulation (C++) (a) 27 March 2017, (b) 28 March 2017, (c) 29 March 2017

Fig. 10 shows the absorber plate temperature for the new cascade solar still with slope surfaces and baffles.

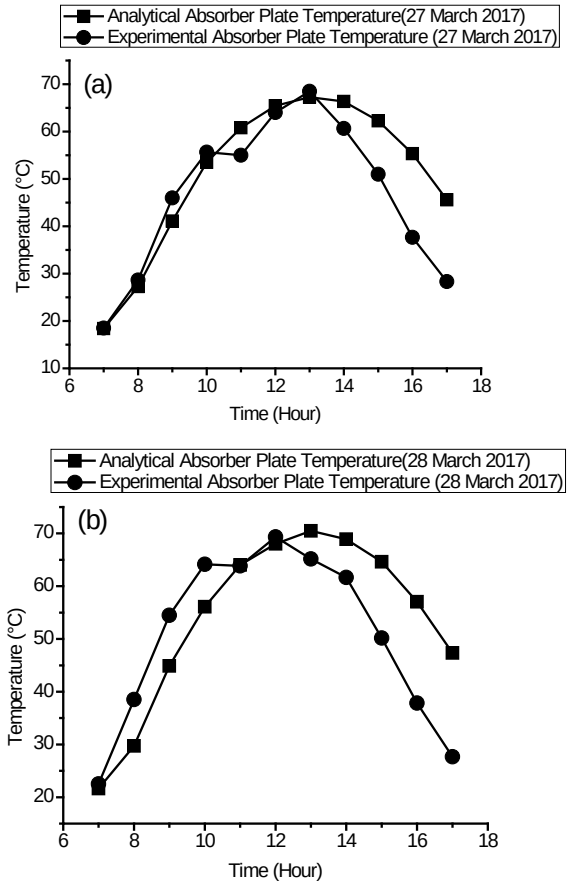

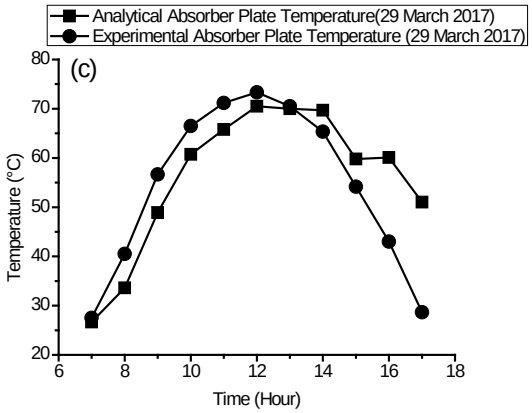

Figure 10: Hourly variation of the analytical and the experimental absorber plate temperature. (a) 27 March 2017, (b) 28 March 2017, (c) 29 March 2017

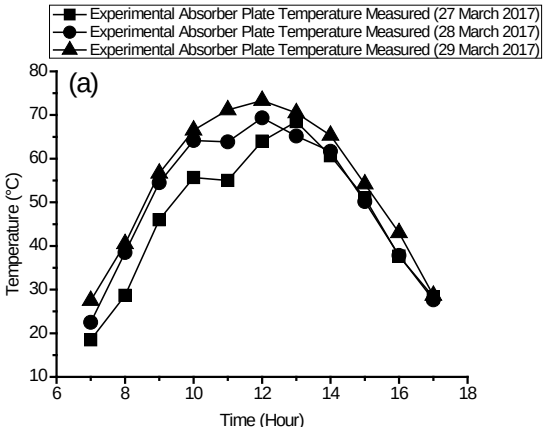

Figure 11: Hourly variation of the experimental absorber plate temperature measured during the three days (27, 28 and 29 March 2017)

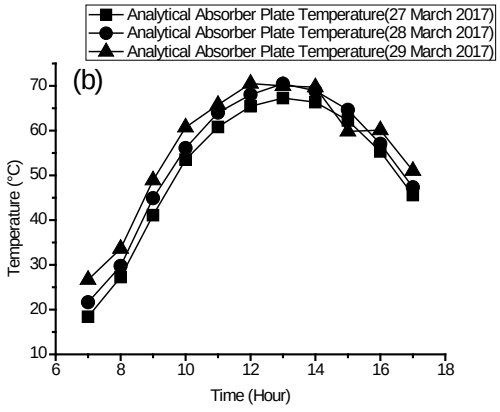

Figure 12: Analytical results of the absorber plate temperature for the three days (27, 28 and 29 March 2017)

To confirm the mathematical model, the variation of the absorber plate temperature is compared with the experimental data of the pattern. As it can be seen from the illustrations there is a good agreement between the analytical method and the experimental results collected on 27, 28 and 29 March 2017. Also the curves of the thermal model programmed in C++ have the same behavior like that of the built model. Fig. 11 and Fig. 12 represent the experimental and the analytical temperature of absorber plate temperature for the three days 27, 28 and 29 March 2017. The absorber plate temperature measured during the experimental process and analytically calculated from the simulation on last day (29/03/2017) are higher than that of the second and the first days. The analytical curves have the same ranking temperatures like that of the experimental data for the three days. Also there was an increase in the temperature during early hours of the day until it reaches the maximum (70°C) after 7 hours of simulation for all days. Fig. 13 shows the variation of hourly productivity with time based on experimental results for the new design of the absorber plate (stepped absorber plate with slope surfaces and weirs).

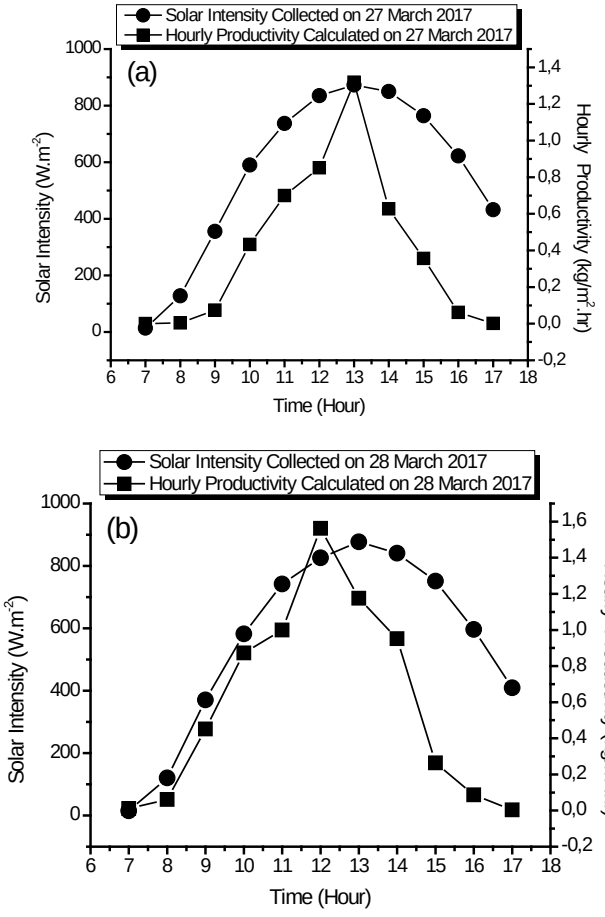

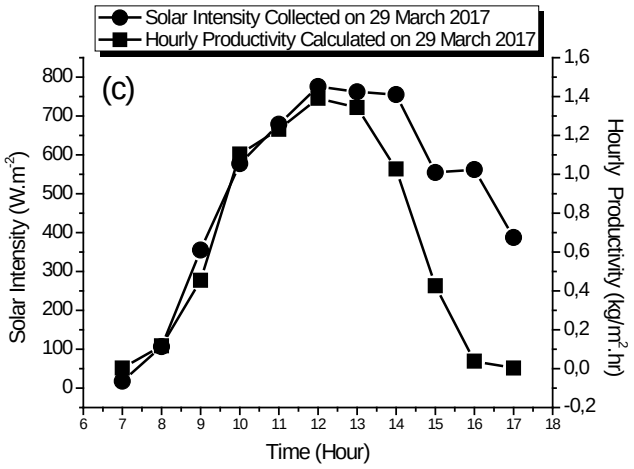

Figure 13: Hourly variation of solar radiation and the hourly productivity of the still. (a) 27 March 2017, (b) 28 March 2017, (c) 29 March 2017

From the Fig. 13, it is found that there was an increase in the water productivity during early hours of the day until it reaches the maximum water productivity around mid-noon during the three days. Also the hourly productivity can reach 1.3 kg/m^2hr for 873 $W.m^{-2}$ of solar intensity in the first day (27 March 2017) Fig. 13(a), 1.5 kg/m^2hr for 826 $W.m^{-2}$ in the second day (28 March 2017) Fig. 13(b) and 1.4 kg/m^2hr for 776 $W.m^{-2}$ in the third day (29 March 2017) Fig. 13(c), which are important values of productivity in comparison with other solar stills results.

7 Conclusion

In this paper, a new type of inclined solar still with stepped absorber plate, slope surfaces and baffles was proposed and tested in order to develop the simple and the cheapest type of desalination. A new pattern of stepped solar still was fabricated and tested during 11 h while three days. A thermal performance of the novel still was investigated and calculated numerically. The energy balance equations are formulated and numerically solved using a simulation program. A comparison was done between simulation results and experimental results of the new absorber plate. The simulation model was tested in order to validate the quality and the capability of the analytical model.

The results show that there is a good agreement between the experimental measures and the calculation which confirms the mathematical model. However there are some differences between the experience and the simulation results due to the losses energetics at the prototype level and the metrological conditions. The results indicate that the new design improves the brackish water and the absorber plate temperature so the thermal performance of a modified stepped solar still can be considerably improved through the new modification. In comparison with other solar still results, the daily production of the new cascade solar still can reach important values, more than 4 kg/m^2day in the first day, 6.43973 kg/m^2 day in the second day and more than 7 kg/m^2dayat the last day.

References

Abdellah, S.; Badran, O.; Abu-Khader, M. M. (2008): Performance evaluation of a modified design of a single slope solar still. *Desalination*, vol. 219, no. 1-3, pp. 222-230.

Abujazar, M. S. S.; Fatihaha, S.; Rakmi, A. R.; Shahrom, M. Z. (2016): The effects of design parameters on productivity performance of a solar still for seawater desalination: A review. *Desalination*, vol. 385, pp. 178-193.

Aggarwal, S.; Tiwari, G. N. (1998): Convective mass transfer in a double-condensing chamber at conventional solar still. *Desalination*, 115, pp. 181-188.

Ali, M. T.; Fath, H. E. S.; Armstrong, P. R. (2011): A comprehensive techno-economical review of indirect solar desalination. *Renewable and Sustainable Energy Reviews*, vol. 15, pp. 4187-4199.

Ansari, O.; Asbik, M.; Bah, A.; Arbaoui, A.; Khmou, A. (2013): Desalination of the brackish water using a passive solar still with a heat. *Desalination*, vol. 324, pp. 10-20.

Aybar, H. S. (2006): Mathematical modeling of an inclined solar water distillation system. *Desalination*, vol. 190, pp. 63-70.

Bouzaid, M.; Oubrek, M.; Ansari, O.; Sabri, A.; Taha-Janan, M. (2016): Mathematical analysis of a new design for cascade solar still performance. *Fluid Dynamics & Materials Processing*, vol. 12, no. 1, pp. 15-32.

Choukr-Allah, R. (2011): Comparative study between moroccan water strategies and WFD. *Options Méditerranéennes*, pp. 181-188.

Cooper, P. I. (1969): Digital simulation of transient solar still processes. *Solar Energy*, vol. 12, pp. 313-331.

Dashtban, M.; Tabrizi, F. F. (2011): Thermal analysis of a weir-type cascade solar still integrated with PCM storage. *Desalination*, vol. 279, pp. 415-422.

Duffie, J. A.; Beckman, W. A. (1980): *Solar Engineering of Thermal Processes*. Wiley, New York, vol. 3, pp. 65.

Dunkle, R. V. (1961): Solar water distillation, the roof type still and a multiple effect diffusion still. *Proceedings of the ASME International Developments in Heat Transfer*, pp. 895-902.

El-Sebaii, A. A. (2005): Thermal performance of a triple-basin solar still. *Desalination*, vol. 174, pp. 23-37.

El-Sebaii, A. A.; Al-Ghamdi, A. A.; Al-Hazmi, F. S.; Faidah, A. S. (2009): Thermal performance of a single basin solar still with PCM as a storage medium. *Applied Energy*, vol. 86, pp. 1187-1195.

Gleck, P. H. (1996): Water resources. In S. H. Schneider Ed., *Encyclopedia of Climate and Weather*. Oxford University Press, New York, vol. 2, pp. 817-823.

Hollands, K. G. T.; Unny, T. E.; Raithby, G. D.; Konicek, L. (1976): Free convective heat transfer across inclined air layers. *Journal of Heat Transfer*, vol. 98, no. 2, pp. 189-193.

Kabeel, A. E.; Khalil, A.; Omara, Z. M.; Younes, M. M. (2012): Theoretical and experimental parametric study of modified stepped solar still. *Desalination*, vol. 289, pp. 12-20.

Kreith, F. (1967): Transmission de la chaleur et thermodynamique. pp. 484-488.

Kumar, S.; Tiwari, G. N. (1985): Estimation of convective mass transfer in solar distillationsystems. *Solar Energy*, vol. 57, pp. 459-464.

Maurel, A. (2006): Dessalement de l'eau de mer et des eaux saumâtres Et autres procédés non conventionnelsd'approvisionnement en eau douce. *Lavoisier/Tec Et Doc*, pp. 199.

Nfaoui, H.; Sayigh, A. A. M. (2015): Contribution of renewable energy to morocco's energy independence. *ISESCO Journal of Science and Technology*, vol. 11, pp. 90-96.

Radhwan, A. M. (2004): Transient analysis of a stepped solar still for heating and humidifying greenhouses. *Desalination*, vol. 161, pp. 89-97.

Sathyamurthy, R.; Harrris Samuel, D. G.; Nagarajan, P. K.; Jaiganesh, V. (2015); Experimental investigation of a semi-circular trough solar water heater. *Applied Solar Energy*, vol. 51, no. 2, pp. 94-98.

Sathyamurthy, R.; Samuel, D. G. H.; Nagarajan, P. K. (2015): Theoretical analysis of inclined solar still with baffle plates for improving the fresh water yield. *Process Safety and Environmental Protection* vol. 101, no. 3, pp. 93-107.

Shannon, M. A.; Bohn, P. W.; Elimelech, M.; Georgiadis, J. G.; Marinas, B. J. et al. (2008): Science and technology for water purification in the coming decades. *Nature Publishing Group*, vol. 452, pp. 301-310.

Sharshir, S. W.; Yang, N.; Peng, G.; Kabeel, A. E. (2016): Factors affecting solar stills productivity and improvement techniques: A detailed review. *Applied Thermal Engineering*, vol. 100, pp. 267-284.

Singh, H. N.; Tiwari, G. N. (2004): Monthly performance of passive and active solar stills for different Indian climatic condition. *Desalination*, vol. 168, pp. 145-150.

Singh, S. K.; Tiwari, G. N. (1991); Analytical expression of thermal efficiency of a passive solar still. *Energy Convers Manage*, vol. 22, no. 6, pp. 571-576.

Tiwari, A. K.; Tiwari, G. N. (2006): Effect of water depths on heat and mass transfer in a passive solar still: In summer climatic condition. *Desalination*, vol. 195, pp. 78-94.

Tiwari, G. N. (1987): Effect of water depth on daily yield of the still. *Desalination*, vol. 61, no. 1, pp. 67-75.

Tiwari, G. N. (2002): *Solar Energy: Fundamentals, Design, Modelling and Application*. CRC Press, New York.

Tiwari, G. N.; Lawrence, S. A.; Gupta, S. P. (1989): Analytical study of multi-effect solar still. *Energy Conversion and Management*, vol. 29, no. 4, pp. 259-263.

Tiwari, G. N.; Madhuri (1987): Effect of water depth on daily yield of the still. *Desalination*, vol. 61, pp. 67-75.

Velmurugan, V.; Kumar, K. J. N.; Haq, T. N.; Srithar, K. (2009): Performance analysis in stepped solar still for effluent desalination. *Energy*, vol. 34, pp. 1179-1186.

Velmurugana, V.; Srithar, K. (2011): Performance analysis of solar stills based on various factors affecting the productivity-a review. *Renewable & Sustainable Energy Reviews*, vol. 15, pp. 1294-1304.